Check for updates

*Comprehensive Physiology*

SPECIAL ISSUE Microbiome: A Critical Modulator of Multiple Organ Cross Talk in Health and Disease

COMPREHENSIVE PHYSIOLOGY Interorgan communication in health and disease

american physiological society

RESEARCH ARTICLE OPEN ACCESS

# Cross-Sectional Associations Between Gut Microbiota and Neuroimaging Changes in Post-COVID-19 Condition

Sophie Wetz[1] | Ravi Dadsena[1,2] | Nicole Treichel[3] | Ana S. Costa[1,2] | Anna Hofmann[4,5] | Sandro Romanzetti[1,2] | Thomas Clavel[3] | Kathrin Reetz[1,2] | Julia Walders[1,2]

[1]Department of Neurology, RWTH Aachen University, Aachen, Germany | [2]JARA-BRAIN Institute Translational Neuroscience, Forschungszentrum Jülich GmbH and RWTH Aachen University, Aachen, Germany | [3]Functional Microbiome Research Group, Institute of Medical Microbiology, University Hospital RWTH Aachen, Aachen, Germany | [4]German Center for Neurodegenerative Diseases (DZNE), Tübingen, Germany | [5]Department of Cellular Neurology, Hertie Institute for Clinical Brain Research, University Hospital Tübingen, Tübingen, Germany

**Correspondence:** Kathrin Reetz (kreetz@ukaachen.de)

**Received:** 31 March 2026 | **Revised:** 28 August 2026 | **Accepted:** 5 September 2026

**Keywords:** 16S rRNA gene amplicon sequencing | gut dysbiosis | gut-brain axis | neuroimaging | post-COVID-19 condition

## ABSTRACT

**Aim:** Neurological symptoms, including cognitive complaints and fatigue, are common in post-COVID-19 Condition (PCC), a complex multisystem disorder following SARS-CoV-2 infection. Although gut microbiota changes have been reported in PCC and linked to PCC-associated neurological manifestations, its relationship to structural or functional brain changes remains unexplored.

**Methods:** In this cross-sectional study, the gut microbiota composition of 42 post-COVID patients (29 females, 46.7 ± 11.3 years) and 30 healthy controls (22 females, 53.9 ± 17.8 years) was analyzed using 16S rRNA gene amplicon sequencing. Taxa that differed significantly in relative abundance, determined by linear discriminant analysis, were examined for their associations with self-reported symptoms, neuropsychological measures, inflammatory and neuronal-injury markers. Previously identified structural and functional brain changes in post-COVID patients using magnetic resonance imaging were further correlated with relevant taxa.

**Results:** At 9 months post-infection, gut microbiota differed significantly from that of healthy controls. We found a lower relative abundance of butyrate-producing taxa. A lower relative abundance of *Blautia faecis* and *Anaerobutyricum hallii* was linked to diabetes. *Bilophila wadsworthia* was associated with lower sleep quality and cognitive fatigue. *B. wadsworthia*, *Odoribacter splanchnicus*, *Coprococcus eutactus*, and *Streptococcus thermophilus* were associated with altered structural and functional brain regions, including the brainstem, the thalamus, the hippocampus and the basal ganglia.

**Conclusion:** Our study provides evidence linking microbiota dysbiosis in PCC to symptoms and cerebral alterations, possibly related to depletion of health-promoting taxa. Future research should investigate the causality of these findings and explore whether microbiome-targeted therapeutic interventions might be associated with improvements in neurological symptoms and brain recovery.

## 1 | Introduction

Post-COVID-19 condition (PCC) has emerged as a significant health concern affecting approximately 5%–10% of individuals after acute SARS-CoV-2 infection (Hastie et al. 2023). PCC is defined by a wide range of symptoms persisting for more than 12 weeks. PCC is associated with a substantial neurological burden including fatigue as the most frequently reported symptom, and cognitive deficits (Elboraay et al. 2025). Due to the high abundance of SARS-CoV-2 cell entry receptor ACE-2

This is an open access article under the terms of the Creative Commons Attribution License, which permits use, distribution and reproduction in any medium, provided the original work is properly cited.

© 2026 The Author(s). *Comprehensive Physiology* published by Wiley Periodicals LLC on behalf of American Physiological Society.

in intestinal epithelia, the gut is particularly vulnerable to viral infection (Paužuolis et al. 2024). Gastrointestinal symptoms appear in nearly half of all patients during the acute phase of COVID-19, i.e., up to 4 weeks after infection and shedding of SARS-CoV-2 in feces can persist up to 7 months after COVID-19 (Jones et al. 2020; Natarajan et al. 2022; Hossain et al. 2023). Given its crucial role in supporting a robust immune system, the disruption of the gut microbiome has therefore emerged as one hypothesized mechanism contributing to PCC disease pathogenesis (Davis et al. 2023).

Recent studies have underscored the importance of the gut-brain axis in PCC, building upon its well-established role in neuropsychiatric diseases (Cryan et al. 2019). Several studies found a significantly altered gut microbiota composition in both patients with acute COVID-19 and as well as patients with PCC compared to healthy controls (Yeoh et al. 2021; Liu et al. 2022; Su et al. 2023). Gut microbiota composition was found to be associated with COVID-19 disease severity and dysfunctional immune responses (Yeoh et al. 2021). Patients with pre-existing conditions, such as obesity and Type 2 diabetes, that are also causally associated with gut microbiome changes are at higher risk of developing severe COVID-19 (Zhou et al. 2021; Tseng and Wu 2019; Zhou et al. 2022). In PCC patients, cross-sectional and longitudinal studies have revealed microbiome aberrations related to self-reported symptoms (Yeoh et al. 2021; Liu et al. 2022; Su et al. 2024). For instance, neuropsychiatric symptoms and fatigue have been correlated with nosocomial infections by *Clostridium innocuum* and *Actinomyces naeslundii* (Liu et al. 2022). More specifically, higher levels of *Mediterraneibacter gnavus* (formerly *Ruminococcus gnavus*) and *Phocaeicola vulgatus* (formerly *Bacteroides vulgatus*), along with lower levels of butyrate-producing *Faecalibacterium prausnitzii*, were found to be associated with neurological symptoms and fatigue (Yeoh et al. 2021; Liu et al. 2022).

On a pathomechanistic level, one study has suggested that interferon I-mediated inflammation in the gut may lead to serotonin deficiency and dysfunction of the brainstem and vagus nerve (Wong et al. 2023). Given its crucial role in modulating serotonin biosynthesis, microbiome alterations due to inflammation could lead to impaired vagus nerve signaling between the enteric and central nervous systems and thereby mediate neurological symptoms in PCC. Notably, microstructural alterations in the brainstem have been observed after COVID-19 and could influence autonomic functions underlying persistent clinical manifestations such as fatigue, dysautonomia, and cognitive dysfunction (Rua et al. 2024). This finding is also supported by a post-mortem proteomic study on brain tissue from deceased COVID-19 patients, which found evidence of systemic inflammation affecting the brainstem during the acute stage of the disease (Radke et al. 2024). Along with brainstem changes, functional and structural alterations in the cerebellum, the basal ganglia, the thalamus, the hippocampus, and orbitofrontal areas were also frequently reported after acute COVID-19 (Rua et al. 2024; Dadsena, Walders, et al. 2025; Bungenberg et al. 2024; Radke et al. 2024; Douaud et al. 2022). However, despite these intriguing connections, no study to date has investigated the relationship between microbiota profiles and brain changes in patients with PCC.

We aim to bridge this gap and hypothesize that altered gut microbiomes in PCC patients are linked not only to neurological symptoms but also to structural and functional brain changes, particularly within the brainstem. Understanding the potential contribution of a disrupted microbiome to brain changes in PCC could enhance biological insights into the pathogenesis of this complex condition and open new avenues for therapeutic interventions.

## 2 | Methods

### 2.1 | Study Participants

The study participants for the PCC cohort were recruited at the Department of Neurology at the University Hospital RWTH Aachen. Study participants were considered eligible for inclusion in the study if they were 18 years of age or older and exhibited persistent predominantly neurological symptoms following a confirmed SARS-CoV-2 infection, as determined by reverse transcription polymerase chain reaction (PCR) of nasopharyngeal swab or the presence of antibodies against SARS-CoV-2, with no vaccination prior to the infection. Exclusion criteria for undergoing magnetic resonance imaging (MRI) were contraindications associated with research MRI, such as the presence of metallic implants or claustrophobia. Both patients who had been hospitalized during the acute phase of SARS-CoV-2 infection and non-hospitalized patients were included.

Information about diet was collected via a structured questionnaire.

Approval for all procedures was obtained from the local ethics committee ("Ethikkommission an der Medizinischen Fakultät der RWTH Aachen") and followed the Declaration of Helsinki (EK 192/20). All individuals gave written informed consent before participating in the study. MRI data from matched healthy controls were sourced from prior research projects within our group utilizing identical imaging protocols and the same PRISMA scanner (3T field strength from Siemens, Erlangen, Germany), collected before the onset of the COVID-19 pandemic. Exclusion criteria for healthy controls were neurological or psychiatric comorbidities affecting cerebral health, pregnancy, and severe adipositas.

Stool sample data from healthy controls in Germany, collected before the onset of the COVID-19 pandemic, were obtained from a study performed by Schmiester et al. (BioProject accession number PRJNA782417) (Schmiester et al. 2022). The healthy controls included in this study did not present a history of gastrointestinal inflammatory disease and did not take antibiotics prior to participation. The composition of the control groups for MRI and microbiome data is shown in supplemental Figure S4.

### 2.2 | Clinical Measures

All PCC patients underwent a neurological examination and a comprehensive medical history assessment, as previously outlined (Bungenberg et al. 2022; Heine et al. 2023). Standardized patient reported outcome measures (PROMs) included: the Fatigue Scale



20404603, 2026, 5, Downloaded from https://onlinelibrary.wiley.com/doi/10.1002/cph4.70261 by Universitatsbibliothek RWTH Aachen University, Wiley Online Library on [13/11/2026]. See the Terms and Conditions (https://onlinelibrary.wiley.com/terms-and-conditions) on Wiley Online Library for rules of use; OA articles are governed by the applicable Creative Commons License

for Motor and Cognitive Functions (FSMC), the Hospital Anxiety and Depression Scale (HADS-D), the Epworth Sleepiness Scale (ESS), and the Pittsburgh Sleep Quality Index (PSQI).

The FSMC assesses fatigue on 20 items using a 5-point Likert Scale, distinguishing between physical and cognitive symptoms with a maximum score of 100 (Penner et al. 2009). The overall score and subscales include cut-offs for mild (≥43), moderate (≥53), and severe fatigue (≥63).

For HADS-D, the maximum score for anxiety and depression is set at 21. Severity thresholds were considered for both subscales: ≤7 for normal, 8–10 for questionable, and ≥10 for increased (Herrmann and Buss 1994).

ESS and PSQI assessed symptoms and severity of daytime sleepiness and sleep quality. For ESS, category 0–7 indicates unlikely abnormal sleepiness, 8–9 suggests an average amount of daytime sleepiness, 10–15 implies potential excessive sleepiness, and 16 up to the maximum of 24 signals excessive sleepiness requiring medical attention. For PSQI, the maximum score is 21, whereas a cut-off value of 5 is applied to divide the study cohort into "good" and "poor" sleepers.

### 2.3 | Neuropsychological Assessment

Montreal Cognitive Assessment (MoCA) was used as a measure of global cognition, with a maximum score of 30 (Nasreddine et al. 2005). The comprehensive neuropsychological assessment protocol included common standardized measures of attention, information processing, and psychomotor speed (Trail Making Test-A, TMT-A; Alertness subtests of the Test of Attentional Performance, TAP), executive functions (Stroop Test, phonemic and semantic verbal fluency, Digit span backward, TMT-B), language (Naming, phonemic and semantic verbal fluency), visuospatial processing (Rey-Osterrieth Complex Figure copy, ROCF), memory and learning (Complex Figure delayed recall, Digit span forward, Rey Auditory Verbal Learning Test, RAVLT) (Dadsena, Walders, et al. 2025).

Impairment was characterized as a performance falling below the 16th percentile rank (PR) or between −2 and −1.5 for the z-score, and severe impairment was designated as a PR below 2 or a z-score below −2 (Guilmette et al. 2020). The neuropsychological assessment was only performed in the PCC cohort. The classification of cognitive performance was determined based on published normative data, which took into account factors such as age, level of education, and/or sex, depending on the specific test (Vakil et al. 2010; Tombaugh 2004; Bäumler 1985; Aschenbrenner et al. 2000; Petermann 2014; Russ 2001; Zimmermann and Fimm 2017).

### 2.4 | Sample Collection and High-Throughput 16S rRNA Gene Amplicon Sequencing

Stool samples were collected by providing the study participants with 1000 ML containers (Corning Gosselin, art. Nr. 216-4278), including a sterile plastic bag (Stomacher 400, art. Nr. 432-3126) and an anaerobic generator (BD GasPak EZ Anaerobier Pouch System, Art. Nr. 260683). The participants were instructed to defecate into a plastic bag placed in a container, fold the plastic bag, put the anaerobic generator on the folded plastic bag and close the container with the lid. The samples were stored at room temperature and processed within 24 h after defecation. After homogenization by kneading the plastic bag manually, the samples were aliquoted by filling approximately half of a 1.5 ML Eppendorf tube (Art. Nr. 0030120086) with the fecal matter, mixing it with 600 μL of RNA*later* Stabilization Solution (Sigma Aldrich, art. Nr. R0901-500ML) and then stored at −80°C until further processing. DNA isolation and 16S rRNA gene amplicon sequencing (V3-V4 regions) were performed as previously described (Afrizal et al. 2022).

Raw 16S rRNA gene amplicon sequencing paired-end reads were processed using the online platform IMNGS based on the UPARSE analysis pipeline (Lagkouvardos et al. 2016; Edgar 2013). Default filtering parameters were applied. With IMNGS, pairing, quality filtering and clustering of Operational taxonomic units (OTUs) at 97% sequence similarity was performed using USEARCH (Edgar 2010). The presence of chimeras in these OTUs was checked using UCHIME (Edgar et al. 2011). Taxonomic classification was performed by SINA v1.6.1, using the taxonomy of SILVA release 128 (Pruesse et al. 2012). Phylogenetic tree was calculated by Fasttree using maximum likelihood-approximation (Price et al. 2010). Further data processing was performed in R (version R 4.3.3) using the packages *Rhea, phyloseq* (version 1.46.0), *microbiomeMarker* (1.8.0) and *vegan* (version 2.6.4) (McMurdie and Holmes 2013; Cao et al. 2022; Oksanen et al. 2022; Lagkouvardos et al. 2017). OTUs with a relative abundance < 0.25% were removed (Reitmeier et al. 2021). Further sequence identification of relevant OTUs was performed using EzBioCloud (Chalita et al. 2024).

### 2.5 | Blood Markers

Blood samples were analyzed by our in-house laboratory at the UKA and included c-reactive protein (CRP), interleukin 2 (IL-2), interleukin 6 (IL 6), interleukin 8 (IL 8), interleukin 10 (IL-10), interleukin 2 receptor (IL-2R), tumor necrosis factor alpha (TNF-α), procalcitonin (PCT) and ferritin (FERR). Neurofilament light (NFL) and Glial fibrillary acidic protein (GFAP) were measured utilizing a commercially available assay kits on the SIMOA HD-X platform at the Hertie Institute for Clinical Brain Research in Tübingen, Germany as previously described (Dadsena, Wetz, et al. 2025).

### 2.6 | MRI Analysis

MRI imaging data acquisition, processing, and analysis of structural and functional MRI data are described in detail in our previous work (Dadsena, Wetz, et al. 2025; Dadsena, Walders, et al. 2025). In brief, MRI was acquired on 3-T Siemens PRISMA scanners using high-resolution T1-weighted imaging and eyes-open functional resting-state MRI. Data underwent automated and visual quality control, motion assessment, and standardized preprocessing. Structural images were analyzed using FastSurfer or CAT12 to derive regional morphometric measures. Resting-state data were processed with fMRIPrep, denoised, spatially normalized, and analyzed for regional activity and functional connectivity.



20404603, 2026, 5, Downloaded from https://onlinelibrary.wiley.com/doi/10.1002/cph4.70261 by Universitatsbibliothek RWTH Aachen University, Wiley Online Library on [13/11/2026]. See the Terms and Conditions (https://onlinelibrary.wiley.com/terms-and-conditions) on Wiley Online Library for rules of use; OA articles are governed by the applicable Creative Commons License

## 2.7 | Statistical Analysis

*Alpha*-diversity was calculated as Shannon effective counts, as previously described (Lagkouvardos et al. 2017). *Beta*-diversity was computed based on weighted UniFrac distances. PERMANOVA was performed using the adonis function from the vegan package. We performed Linear discriminant analysis Effect Size (LEfSe) with the *microbiomeMarker* package to identify discriminatory taxa, for simplicity here referred to as "microbial markers" (Segata et al. 2011). These markers were corrected for age and sex and further used for correlation analyses. Pearson correlation coefficients were calculated for binary variables. Spearman correlation coefficient was calculated for ordinal variables and non-normally distributed numeric variables. The coefficients are reported with unadjusted *p*-values, setting the significance level at $p < 0.05$. Given the exploratory nature of the analysis and the high dimensionality of microbiome data, non-adjusted *p*-values are reported to identify potential trends. For the correlation analysis of structural and functional brain changes, we focused on regions we identified as significantly altered in our previous neuroimaging studies within this cohort, which included the right amygdala, the brainstem, the right and left lateral ventricle, the left ventral diencephalon, the right and left medial segment of postcentral gyrus for structural brain changes, and the right cingulate gyrus, the left orbital gyrus, the caudal area and entorhinal cortex of the left parahippocampal gyrus, and left postcentral gyrus for functional brain changes (Dadsena, Walders, et al. 2025; Dadsena, Wetz, et al. 2025). The volumetric scores for structural brain changes and *z*-scores for functional brain changes were correlated with the center-log ratio transformed abundance of previously identified microbial markers. A prevalence threshold of approximately 33% (14 out of 42 samples) was applied. Taxonomic zeros were replaced with missing values due to the compositional nature of the data (Aitchison 1982). Correlation heatmaps were created with the R package *MicroViz* (Barnett et al. 2021).

# 3 | Results

## 3.1 | Epidemiological and Clinical Characteristics

Characteristics of study participants are shown in Table 1. The cohort of 42 patients was primarily female (69.04%), with a mean age of 46.7 ± 11.3 years and had a primarily omnivorous diet (74%). Nine patients were hospitalized during the acute infection, including five who required intensive care. The time interval between initial SARS-CoV-2 infection and study participation including fecal sample collection was 9.2 ± 4.2 months. The majority presented moderate to severe fatigue (20.5% and 46.1%, respectively, based on FSMC) and poor sleep (72.2%, based on PSQI). Affective symptoms were less prominent according to the HADS, with 66.6% and 84.6% of the study cohort being within the normal range for anxiety and depression, respectively. Additionally, most frequently self-reported symptoms included attention and concentration problems, word finding problems, as well as smell and taste disturbances (Figure S1A). Overall, blood marker levels were within the normal reference ranges and are shown in Table 2. In the neuropsychological assessment, attention was most often affected, followed by executive functions and learning and memory (Figure S1B). In the

**TABLE 1** | Clinical and demographic characteristics of study participants with post-COVID-19 Condition.

| Variable | Value |
|---|---|
| PCC patients | 42 |
| Female sex | 29 (69.0%) |
| Age (years) | 46.7 ± 11.3 |
| Months after infection | 9.2 ± 4.2 |
| Mild Cognitive Impairment | 15 (35.7%) |
| Cardiovascular risk factors | |
| Hypertension | 7 (16.7%) |
| Diabetes mellitus | 3 (7.1%) |
| Dyslipidemia | 1 (2.4%) |
| Overweight (BMI ≥ 30 kg/m$^2$) | 9 (21.4%) |
| BMI (kg/m$^2$) | 25.7 ± 5.0 |
| Hospitalization | 9 (21.4%) |
| Intensive Care Unit | 5 (12.0%) |
| Days hospitalized | 33.6 ± 16.9 |
| Diet | |
| Omnivorous | 31 (73.8%) |
| Vegetarian | 4 (9.5%) |
| Vegan | 2 (4.8%) |
| Other/Unknown | 5 (11.9%) |
| Fatigue (FSMC) | |
| None | 6 (15.4%) |
| Mild | 7 (18.0%) |
| Moderate | 8 (20.5%) |
| Severe | 18 (46.1%) |
| Daytime Sleepiness (ESS) | |
| None | 23 (62.2%) |
| Average | 3 (8.1%) |
| Potentially excessive | 8 (21.6%) |
| Excessive | 3 (8.1%) |
| Sleep quality (PSQI) | |
| Poor | 26 (72.2%) |
| Good | 10 (27.8%) |
| Anxiety (HADS-D) | |
| Normal | 26 (66.6%) |
| Questionable | 7 (18.0%) |
| Increased | 6 (15.4%) |

(Continues)



20404603, 2026, 5, Downloaded from https://onlinelibrary.wiley.com/doi/10.1002/cph4.70261 by Universitatsbibliothek RWTH Aachen University, Wiley Online Library on [13/11/2026]. See the Terms and Conditions (https://onlinelibrary.wiley.com/terms-and-conditions) on Wiley Online Library for rules of use; OA articles are governed by the applicable Creative Commons License

**TABLE 1** | (Continued)

| Variable | Value |
|---|---|
| Depression (HADS-D) | |
| Normal | 33 (84.6%) |
| Questionable | 4 (10.3%) |
| Increased | 2 (5.1%) |

*Note:* Data presented as mean (standard deviation) or *n* (%).
Abbreviations: BMI, Body Mass Index; ESS, Epworth sleepiness scale; FSMC, Fatigue Scale for Motor and Cognitive Function; HADS-D, Hospital Anxiety and Depression scale; PCC, post-COVID-19 Condition; PSQI, Pittsburgh Sleep Quality Index.

**TABLE 2** | Overview of fluid markers results of study participants with post-COVID-19 condition.

| Parameter (unit) | N | Mean ± SD | Reference range |
|---|---|---|---|
| CRP (mg/L) | 40 | 2.04 ± 2.63 | < 5 |
| IL-10 (pg/mL) | 41 | 4.74 ± 21.35 | < 9.1 |
| IL-2 (pg/mL) | 39 | 1.21 ± 0.84 | < 5.0 |
| IL-2R (U/mL) | 41 | 341.79 ± 172.30 | 223–710 |
| IL-6 (pg/mL) | 42 | 2.36 ± 1.75 | < 7.0 |
| IL-8 (pg/mL) | 41 | 9.46 ± 9.66 | < 62 |
| PCT (ng/mL) | 42 | 0.034 ± 0.031 | < 0.5 |
| TNF-α (pg/mL) | 42 | 5.98 ± 3.61 | < 8.1 |
| NfL (pg/mL) | 41 | 10.45 ± 16.49 | < 15 |
| GFAP (pg/mL) | 41 | 169.04 ± 406.32 | < 242 |
| Ferritin (ng/mL) | 41 | 147.44 ± 369.48 | 15.0–150 |

*Note:* Data are given as mean with standard deviation (SD).
Abbreviations: CRP, C-reactive protein; GFAP, Glial fibrillary acidic protein; IL, Interleukin; NfL, Neurofilament light; PCT, Procalcitonin; R, receptors; TNF-α, Tumor necrosis factor-alpha.

healthy cohort for the microbiome analysis, 22 out of 30 participants were female (73%), with a mean age of 53.9 ± 17.8 years.

### 3.2 | Gut Microbiota Shifts in PCC Patients

*Alpha*-diversity analysis revealed no significant difference in the PCC group compared to the healthy control group (Figure 1A). *Beta*-diversity analysis showed significantly different phylogenetic profiles of the microbiota between the two groups (Figure 1B, PERMANOVA, $p < 0.001$). Within the PCC group, there was no significant difference in *alpha*- and *beta*-diversity between hospitalized and non-hospitalized patients (*alpha*-diversity: *t*-test, $p > 0.05$; *beta*-diversity: PERMANOVA, $p = 0.424$). Lefse analysis of single OTUs revealed significant microbial markers, which were used for subsequent analyses (Figure 1C). The taxa names with best identity match to the OTU sequences are listed in Table 3. The top taxa for the healthy control group included species of the genus *Blautia* (OTU_1: *B. luti*; OTU_5: *B. massiliensis*; OTU_324: *B. obeum*; OTU_161: *B. faecis*), *Agathobacter rectalis* (OTU_2), *Fusicatenibacter saccharivorans* (OTU_3), and *Coprococcus eutactus* (OTU_41). In the PCC group, the top taxa included multiple species of the genus *Phocaeicola* (formerly *Bacteroides*) (OTU_9414: *P. vulgatus*; OTU_11: *P. dorei*; OTU_1013: *P. ovatus*), PAC001129_s within the genus *Vescimonas* (OTU_78), *Alistipes shahii* (OTU_165), and *Parabacteroides merdae* (OTU_47).

### 3.3 | Associations Between Microbial, Clinical, and Blood Markers in the PCC Cohort

Regarding the clinical factors and symptoms reported by the patients, correlation analysis (Figure S2) revealed *B. faecis* (OTU_161) and *Anaerobutyricum hallii* (OTU_15) inversely correlating with Type 2 diabetes. Autonomic dysfunction was positively associated with taxa such as *Coprococcus catus* (OTU_37, $p < 0.05$) and *Odoribacter splanchnicus* (OTU_109, $p < 0.05$).

*Bilophila wadsworthia* (OTU_102) showed positive associations with PROMs (Figure 2) related to sleep (PSQI, $p < 0.01$) and cognitive fatigue (FSMC, $p < 0.05$). *Ruminococcus callidus* (OTU_44) was negatively associated with high FSMC total and cognitive scores, PSQI and total HADS scores ($p < 0.05$). *B. intestinalis* (OTU_1475) was negatively associated with the depression subscore of the HADS ($p < 0.01$) and the PSQI ($p < 0.05$).

For the neuropsychological assessment results (Figure S3), correlation analysis revealed positive associations between PAC001047_s (OTU_285 (*Butyribacter* sp.)) and poor performance in the RAVLT (Trial 5, $p < 0.05$), in tonic and phasic alertness tests ($p < 0.01$). Correlation analyses between microbial, inflammatory, and neuronal injury markers showed only a few associations (Figure 3). Specifically, *R. callidus* (OTU_44) correlated positively with IL-8 ($p < 0.05$), and taxa such as *C. eutactus* (*OTU_41*) and *F. saccharivorans* (OTU_3) correlated positively with GFAP and NfL ($p < 0.05$). IL-6 and IL-8 were both negatively associated with *A. hallii* (OTU_15, $p < 0.001$ and $p < 0.05$, respectively).

### 3.4 | Altered Gut Microbiota Composition Correlated With Structural and Functional Brain Changes in the PCC Cohort

The correlation heatmap (Figure 4A) showed associations between various brain regions and microbial markers enriched or depleted in PCC. Multiple taxa revealed positive correlations with multiple structural brain changes, such as *R. callidus* (OTU_44, depleted in PCC) and *A. hallii* (OTU_15, depleted in PCC), or negative correlations, such as *Alistipes communis* (OTU_143, enriched in PCC). In detail, we found negative correlations between *Odoribacter splanchnicus* (OTU_109, enriched in PCC) and the volumetric score of the right thalamus (Figure 4A, $R = -0.37$, $p < 0.05$), the brainstem (Figure 4A, $R = -0.36$, $p < 0.05$) and the left cerebellar cortex (Figure 4B, $R = -0.42$, $p = 0.019$), *B. wadsworthia* (OTU_102, enriched in PCC) and the right hippocampus (Figure 4C, $R = -0.39$, $p = 0.033$), and *C. eutactus* (OTU_41, enriched in PCC) and the left pallidum (Figure 4D, $R = 0.5$, $p = 0.021$).



20404603, 2026, 5, Downloaded from https://onlinelibrary.wiley.com/doi/10.1002/cph4.70261 by Universitatsbibliothek RWTH Aachen University, Wiley Online Library on [13/11/2026]. See the Terms and Conditions (https://onlinelibrary.wiley.com/terms-and-conditions) on Wiley Online Library for rules of use; OA articles are governed by the applicable Creative Commons License

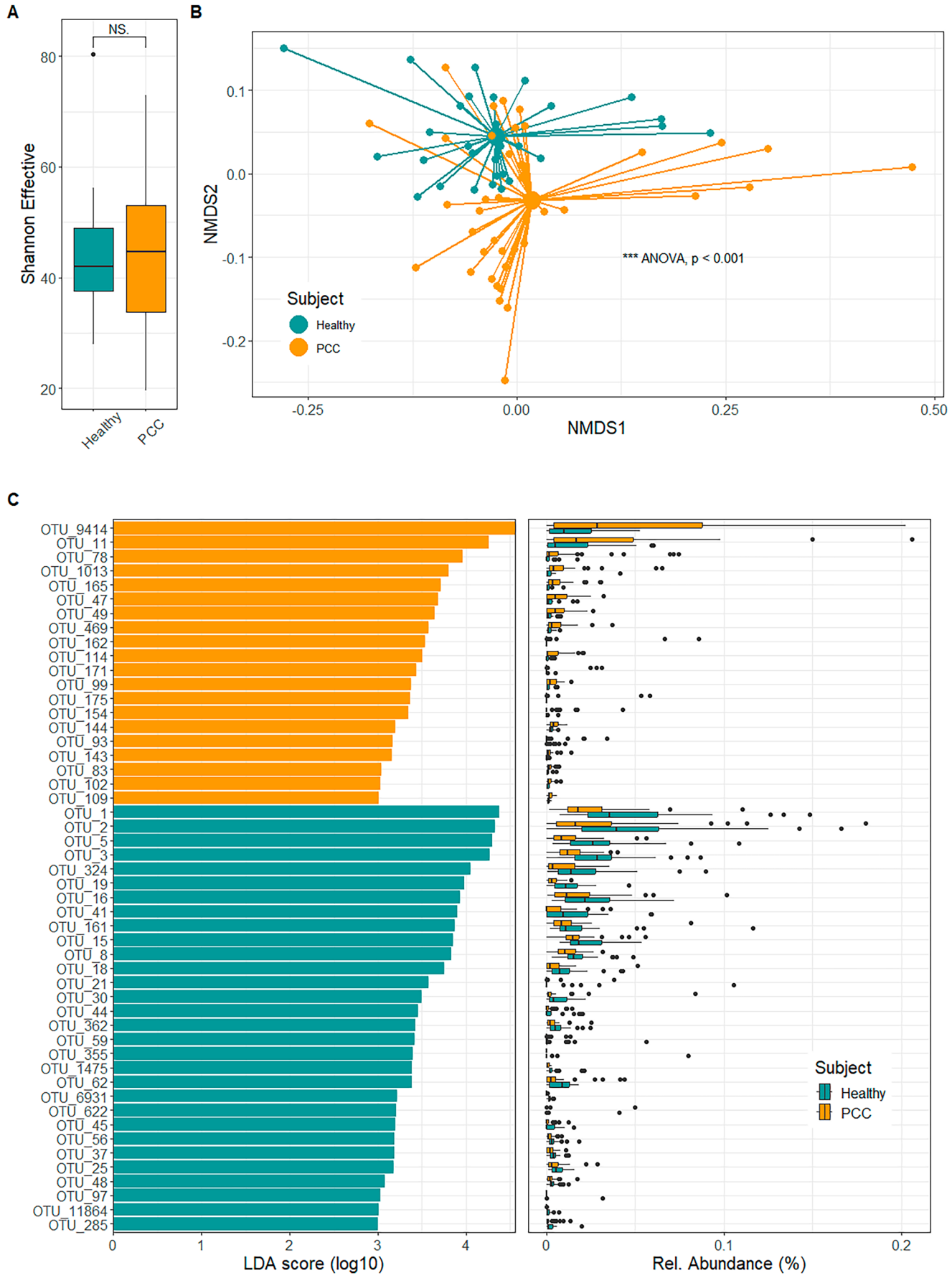



**FIGURE 1** | Legend on next page.



20404603, 2026, 5, Downloaded from https://onlinelibrary.wiley.com/doi/10.1002/cph4.70261 by Universitatsbibliothek RWTH Aachen University, Wiley Online Library on [13/11/2026]. See the Terms and Conditions (https://onlinelibrary.wiley.com/terms-and-conditions) on Wiley Online Library for rules of use; OA articles are governed by the applicable Creative Commons License

**FIGURE 1** | Gut microbiota diversity and composition. (A) Difference in alpha-diversity (Shannon effective) between healthy controls and the PCC study cohort (*t*-test, N.S., no significance). (B) Non-metric multidimensional scaling plot showing differences in beta-diversity between healthy controls and the PCC study cohort based on weighted UniFrac distances (PERMANOVA, $***p < 0.001$). (C) Linear discriminant analysis (LDA) results on single OTU level showing microbial markers for healthy controls and the PCC study cohort. Left: LDA score; Right, relative abundance (%).

**TABLE 3** | Operational taxonomic unit (OTU) look-up table.

| OTU | Top-hit taxon | Top-hit strain | Similarity (%) | Top-hit taxonomy | Completeness (%) |
|---|---|---|---|---|---|
| OTU_1 | *Blautia luti* | DSM 14534 | 100 | *Bacteria*; *Bacillota; Clostridia; Lachnospirales; Lachnospiraceae; Blautia* | 28.2 |
| OTU_2 | *Agathobacter rectalis* | ATCC 33656 | 100 | *Bacteria*; *Bacillota; Clostridia; Lachnospirales; Lachnospiraceae; Agathobacter* | 28.2 |
| OTU_3 | *Fusicatenibacter saccharivorans* | HT03-11 | 100 | *Bacteria*; *Bacillota; Clostridia; Lachnospirales; Lachnospiraceae; Fusicatenibacter* | 28.2 |
| OTU_5 | *Blautia massiliensis* | GD9 | 100 | *Bacteria*; *Bacillota; Clostridia; Lachnospirales; Lachnospiraceae; Blautia* | 28.2 |
| OTU_8 | *Dorea longicatena* | DSM 13814 | 100 | *Bacteria*; *Bacillota; Clostridia; Lachnospirales; Lachnospiraceae; Dorea* | 28.2 |
| OTU_11 | *Phocaeicola (Bacteroides) dorei* | DSM 17855 | 100 | *Bacteria*; *Bacteroidota; Bacteroidia; Bacteroidales; Bacteroidaceae; Phocaeicola* | 29.6 |
| OTU_15 | *Anaerobutyricum hallii* | ATCC 27751 | 100 | *Bacteria*; *Bacillota; Clostridia; Lachnospirales; Lachnospiraceae; Anaerobutyricum* | 28.2 |
| OTU_16 | *Anaerostipes hadrus* | DSM 3319 | 100 | *Bacteria*; *Bacillota; Clostridia; Lachnospirales; Lachnospiraceae; Anaerostipes* | 28.2 |
| OTU_18 | *Faecalibacillus intestinalis* | SNUG30099 | 100 | *Bacteria*; *Bacillota; Erysipelotrichia; Erysipelotrichales; Coprobacillaceae; Faecalibacillus* | 30 |
| OTU_19 | DQ777915_s | R-1263 | 96.59 | *Bacteria*; *Bacillota*; *Clostridia; Lachnospirales; Lachnospiraceae; FMGY_g* | 28.6 |
| OTU_21 | *Dialister hominis* | 5BBH33 | 100 | *Bacteria*; *Bacillota; Negativicutes; Veillonellales; Dialisteraceae; Dialister* | 29.2 |
| OTU_25 | PAC000672_s | | 99.03 | *Bacteria*; *Bacillota; Clostridia; Monoglobales; Monoglobaceae; Hominilimicola* | 28.3 |
| OTU_30 | *Streptococcus thermophilus* | ATCC 19258 | 100 | *Bacteria*; *Bacillota*; *Bacilli; Lactobacillales; Streptococcaceae; Streptococcus* | 29.6 |
| OTU_37 | *Coprococcus catus* | L8 | 100 | *Bacteria*; *Bacillota; Clostridia; Lachnospirales; Lachnospiraceae; Coprococcus_g3* | 28.5 |

(Continues)



20404603, 2026, 5, Downloaded from https://onlinelibrary.wiley.com/doi/10.1002/cph4.70261 by Universitatsbibliothek RWTH Aachen University, Wiley Online Library on [13/11/2026]. See the Terms and Conditions (https://onlinelibrary.wiley.com/terms-and-conditions) on Wiley Online Library for rules of use; OA articles are governed by the applicable Creative Commons License

**TABLE 3** | (Continued)

| OTU | Top-hit taxon | Top-hit strain | Similarity (%) | Top-hit taxonomy | Completeness (%) |
|---|---|---|---|---|---|
| OTU_41 | *Coprococcus eutactus* | ATCC 27759 | 100 | *Bacteria*; *Bacillota; Clostridia; Lachnospirales; Lachnospiraceae; Coprococcus* | 28.5 |
| OTU_44 | *Ruminococcus callidus* | ATCC 27760 | 100 | *Bacteria*; *Bacillota; Clostridia; Clostridiales; Oscillospiraceae; Ruminococcus* | 28.7 |
| OTU_45 | PAC001041_s | | 100 | *Bacteria*; *Actinomycetota; Coriobacteriia; Coriobacteriales; Coriobacteriaceae; PAC001041_g* | 28.6 |
| OTU_47 | *Parabacteroides merdae* | ATCC 43184 | 100 | *Bacteria*; *Bacteroidota; Bacteroidia; Bacteroidales; Tannerellaceae; Parabacteroides* | 29.6 |
| OTU_48 | *Agathobaculum butyriciproducens* | SR79 | 99.76 | *Bacteria*; *Bacillota; Clostridia; Clostridiales; Butyricicoccaceae; Agathobaculum* | 28.4 |
| OTU_49 | JPJG_s | ER4 | 100 | *Bacteria*; *Bacillota; Clostridia; Clostridiales; Oscillospiraceae; Hominicoprocola* | 28.4 |
| OTU_56 | *Eubacterium ramulus* | ATCC 29099 | 100 | *Bacteria*; *Bacillota; Clostridia; Lachnospirales; Lachnospiraceae; Eubacterium_g21* | 28.2 |
| OTU_59 | *Phocaeicola (Bacteroides) clarus* | YIT 12056 | 100 | *Bacteria*; *Bacteroidota; Bacteroidia; Bacteroidales; Bacteroidaceae; Phocaeicola* | 29.7 |
| OTU_62 | *Mediterraneibacter faecis* | Eg2 | 99.76 | *Bacteria*; *Bacillota; Clostridia; Lachnospirales; Lachnospiraceae; Mediterraneibacter* | 28.2 |
| OTU_78 | PAC001129_s | | 100 | *Bacteria*; *Bacillota; Clostridia; Clostridiales; Oscillospiraceae; Vescimonas* | 28.4 |
| OTU_83 | *Dysosmobacter welbionis* | J115 | 100 | *Bacteria*; *Bacillota; Clostridia; Clostridiales; Oscillospiraceae; Dysosmobacter* | 28.4 |
| OTU_93 | PAC001051_s | | 100 | *Bacteria*; *Bacillota; Clostridia; Clostridiales; Oscillospiraceae; Eubacterium_g23* | 28.4 |
| OTU_97 | PAC001039_s | | 95.4 | *Bacteria*; *Bacillota; Negativicutes; Veillonellales; Dialisteraceae; Dialister* | 29.2 |
| OTU_99 | *Dysosmobacter segnis* | BX15 | 100 | *Bacteria*; *Bacillota; Clostridia; Clostridiales; Oscillospiraceae; Marseillibacter* | 28.4 |
| OTU_102 | *Bilophila wadsworthia* | ATCC 49260 | 100 | *Bacteria; Desulfobacterota; Desulfovibrionia; Desulfovibrionales; Desulfovibrionaceae; Bilophila* | 29.6 |
| OTU_109 | *Odoribacter splanchnicus* | DSM 20712 | 99.53 | *Bacteria*; *Bacteroidota; Bacteroidia; Bacteroidales; Odoribacteraceae; Odoribacter* | 29.7 |

(Continues)



20404603, 2026, 5, Downloaded from https://onlinelibrary.wiley.com/doi/10.1002/cph4.70261 by Universitatsbibliothek RWTH Aachen University, Wiley Online Library on [13/11/2026]. See the Terms and Conditions (https://onlinelibrary.wiley.com/terms-and-conditions) on Wiley Online Library for rules of use; OA articles are governed by the applicable Creative Commons License

**TABLE 3** | (Continued)

| OTU | Top-hit taxon | Top-hit strain | Similarity (%) | Top-hit taxonomy | Completeness (%) |
|---|---|---|---|---|---|
| OTU_114 | *Parasutterella excrementihominis* | YIT 11859 | 100 | *Bacteria*; *Pseudomonadota; Betaproteobacteria; Burkholderiales; Sutterellaceae; Parasutterella* | 29.7 |
| OTU_143 | *Alistipes communis* | 5CBH24 | 100 | *Bacteria*; *Bacteroidota; Bacteroidia; Bacteroidales; Rikenellaceae; Alistipes* | 29.4 |
| OTU_144 | QUKV_s | OM08-6BH | 99.02 | *Bacteria*; *Bacillota; Clostridia; Lachnospirales; Lachnospiraceae; Hominiventricola* | 28.2 |
| OTU_154 | PAC001276_s | | 100 | *Bacteria*; *Bacteroidota; Bacteroidia; Bacteroidales; Muribaculaceae; PAC001276_g* | 29.5 |
| OTU_161 | *Blautia faecis* | M7-8 | 99.76 | *Bacteria*; *Bacillota; Clostridia; Lachnospirales; Lachnospiraceae; Blautia* | 28.2 |
| OTU_162 | *Megamonas funiformis* | YIT 11815 | 98.39 | *Bacteria*; *Bacillota; Negativicutes; Selenomonadales; Selenomonadaceae; Megamonas* | 29.6 |
| OTU_165 | *Alistipes shahii* | WAL 8301 | 99.53 | *Bacteria*; *Bacteroidota; Bacteroidia; Bacteroidales; Rikenellaceae; Alistipes* | 29.7 |
| OTU_171 | *Phascolarctobacterium succinatutens* | YIT 12067 | 100 | *Bacteria*; *Bacillota; Negativicutes; Acidaminococcales; Acidaminococcaceae; Phascolarctobacterium* | 27.5 |
| OTU_175 | *Megasphaera massiliensis* | NP3 | 99.77 | *Bacteria*; *Bacillota; Negativicutes; Veillonellales; Megasphaeraceae; Megasphaera* | 29.3 |
| OTU_285 | PAC001047_s | | 99.76 | *Bacteria*; *Bacillota; Clostridia; Lachnospirales; Lachnospiraceae; Butyribacter* | 28.2 |
| OTU_324 | *Blautia obeum* | ATCC 29174 | 99.27 | *Bacteria*; *Bacillota; Clostridia; Lachnospirales; Lachnospiraceae; Blautia* | 28.2 |
| OTU_355 | *Bifidobacterium angulatum* | DSM 20098 | 99.76 | *Bacteria*; *Actinomycetota; Actinomycetia; Bifidobacteriales; Bifidobacteriaceae; Bifidobacterium* | 28.7 |
| OTU_362 | *Oliverpabstia intestinalis* | BSM-380-WT-5A | 99.51 | *Bacteria*; *Bacillota; Clostridia; Lachnospirales; Lachnospiraceae; Oliverpabstia* | 28.2 |
| OTU_469 | *Phocaeicola (Bacteroides) thetaiotaomicron* | VPI-5482 | 99.77 | *Bacteria*; *Bacteroidota; Bacteroidia; Bacteroidales; Bacteroidaceae; Phocaeicola* | 29.7 |
| OTU_622 | *Segatella copri* | CB7 | 97.44 | *Bacteria*; *Bacteroidota; Bacteroidia; Bacteroidales; Prevotellaceae; Segatella* | 29.6 |

(Continues)



20404603, 2026, 5, Downloaded from https://onlinelibrary.wiley.com/doi/10.1002/cph4.70261 by Universitatsbibliothek RWTH Aachen University, Wiley Online Library on [13/11/2026]. See the Terms and Conditions (https://onlinelibrary.wiley.com/terms-and-conditions) on Wiley Online Library for rules of use; OA articles are governed by the applicable Creative Commons License

**TABLE 3** | (Continued)

| OTU | Top-hit taxon | Top-hit strain | Similarity (%) | Top-hit taxonomy | Completeness (%) |
|---|---|---|---|---|---|
| OTU_1013 | *Phocaeicola (Bacteroides) ovatus* | ATCC 8483 | 99.07 | *Bacteria; Bacteroidota; Bacteroidia; Bacteroidales; Bacteroidaceae; Phocaeicola* | 29.6 |
| OTU_1475 | *Blautia intestinalis* | 27–44 | 98.78 | *Bacteria; Bacillota; Clostridia; Lachnospirales; Lachnospiraceae; Blautia* | 28.2 |
| OTU_6931 | *Dorea longicatena* | DSM 13814 | 97.8 | *Bacteria; Bacillota; Clostridia; Lachnospirales; Lachnospiraceae; Dorea* | 28.2 |
| OTU_9414 | *Phocaeicola (Bacteroides) vulgatus* | ATCC 8482 | 99.77 | *Bacteria; Bacteroidota; Bacteroidia; Bacteroidales; Bacteroidaceae; Phocaeicola* | 29.7 |
| OTU_11864 | *Romboutsia timonensis* | Marseille-P326 | 95.6 | *Bacteria; Bacillota; Tissierellia; Peptostreptococcales; Peptostreptococcaceae; Romboutsia* | 28.7 |

*Note:* 16S gene amplicon sequences were identified with EzBioCloud.

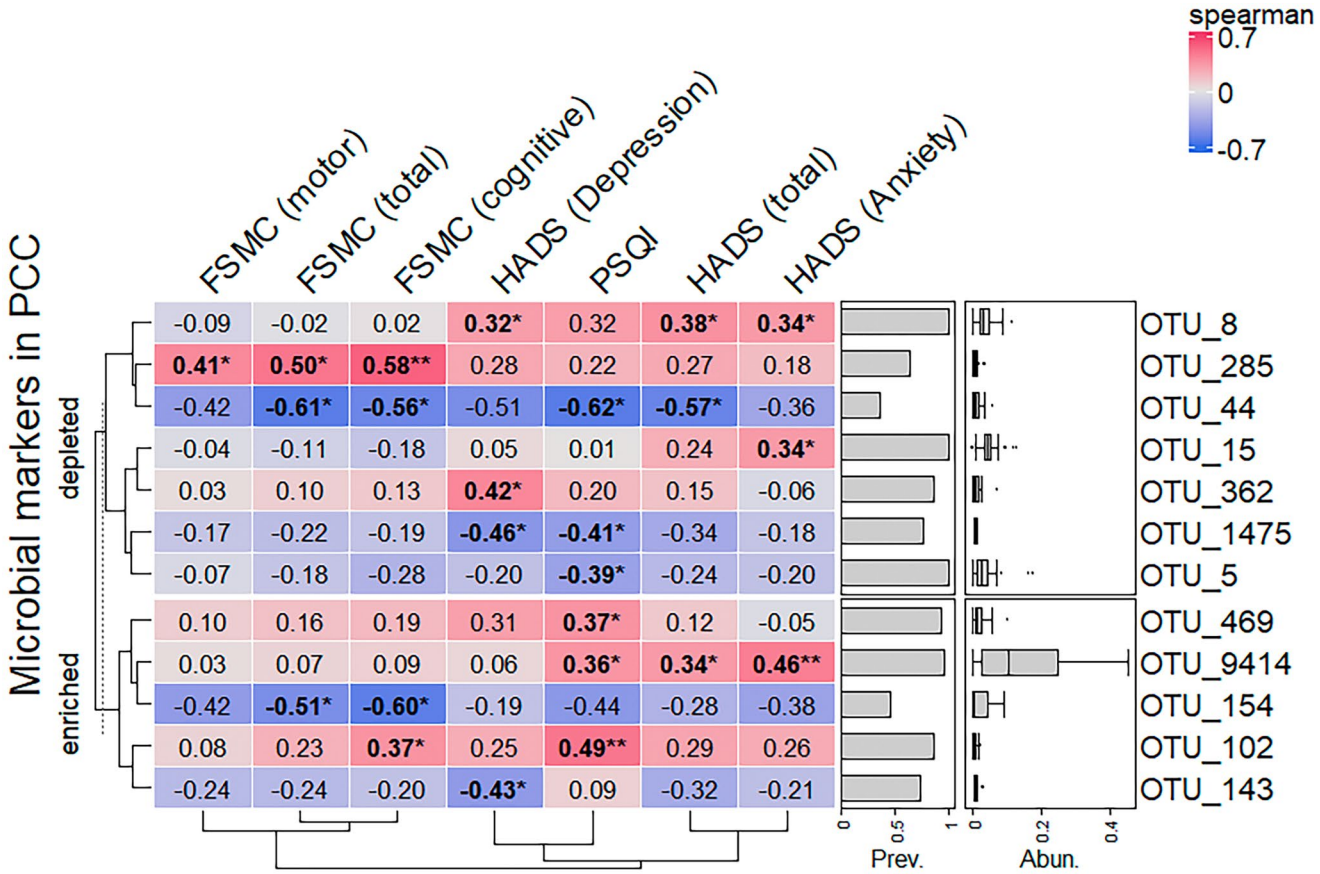



**FIGURE 2** | Correlation analysis results from center-log ratio transformed, relative abundance of microbial taxa and PROM ratings in the PCC cohort. The heatmap shows spearman correlation coefficients and indicating unadjusted significance levels (*$p < 0.05$, **$p < 0.01$).

The same analysis was performed between functional brain imaging data and center-log ratio transformed, relative abundance of microbial taxa (Figure 5). The resulting correlation heatmap revealed positive associations of *Streptococcus thermophilus* (OTU_30, depleted in PCC) with the right caudate (Figure 5A, $R = 0.45$, $p < 0.05$) and in detail, with the left pallidum (Figure 5B, $R = 0.45$, $p = 0.012$). More isolated associations for the remaining microbial taxa included *B. wadsworthia* (OTU_102) and the left



20404603, 2026, 5, Downloaded from https://onlinelibrary.wiley.com/doi/10.1002/cph4.70261 by Universitatsbibliothek RWTH Aachen University, Wiley Online Library on [13/11/2026]. See the Terms and Conditions (https://onlinelibrary.wiley.com/terms-and-conditions) on Wiley Online Library for rules of use; OA articles are governed by the applicable Creative Commons License

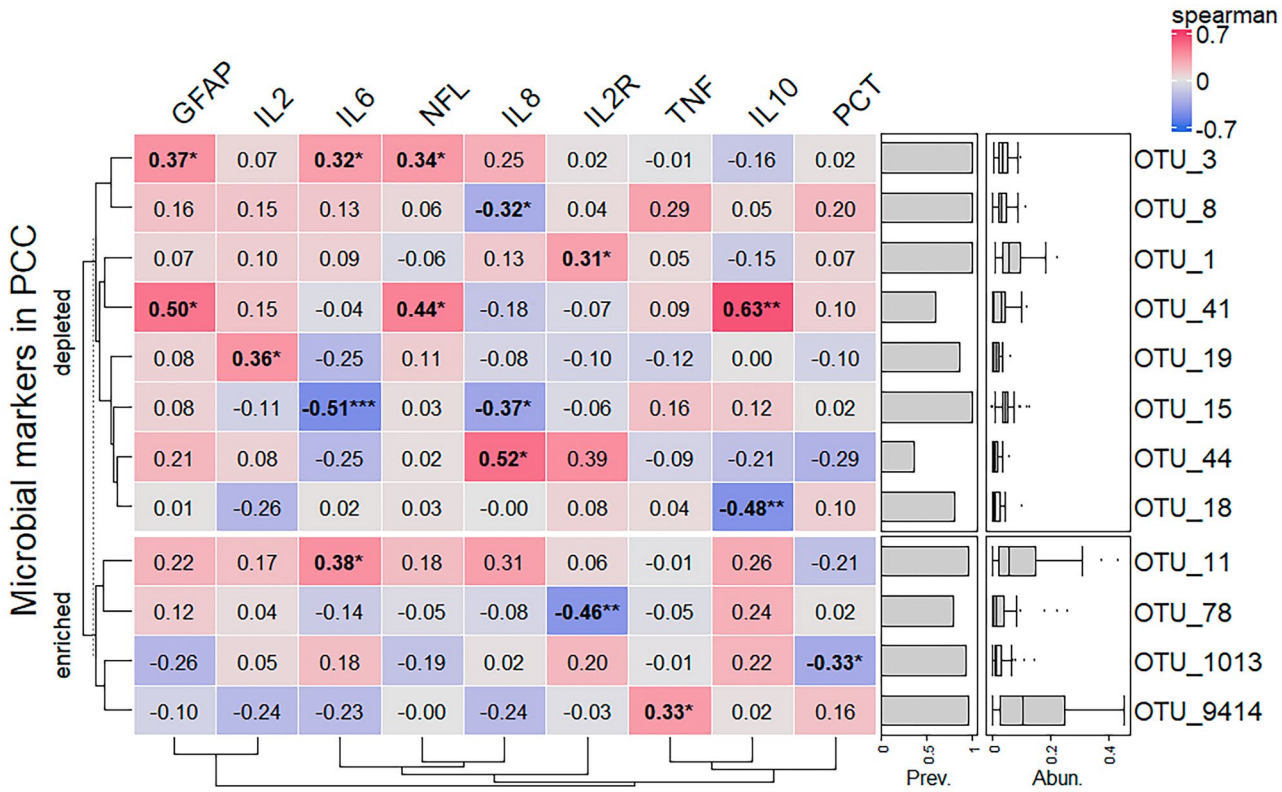



**FIGURE 3** | Correlation analysis results from center-log ratio transformed relative abundance of microbial markers and blood markers in the PCC cohort. The heatmap shows spearman correlation coefficients with asterisks indicating unadjusted significance levels (*$p < 0.05$, **$p < 0.01$, ***$p < 0.001$).

rostral anterior cingulate cortex ($R = 0.46$, $p = 0.015$) (Figure 5C) and *O. splanchnicus* (OTU_109) and the right hippocampus ($R = 0.48$, $p = 0.0099$) (Figure 5D).

## 4 | Discussion

This cross-sectional study investigated potential links between the gut microbiota and clinical, blood, and neuroimaging data in patients with PCC. PCC patients exhibited microbiota alterations linked to clinical measures, including diabetes and cognitive performance, as well as brain changes within the brainstem, the basal ganglia, the hippocampus, and the thalamus.

Reduced microbial diversity in PCC even 1 year after SARS-CoV-2 clearance has previously been described and is considered to be one driver of PCC pathogenesis (Davis et al. 2023; Su et al. 2023; Lau et al. 2025). While we did not observe significant differences in microbial diversity in our cohort, we found increased relative abundances of multiple taxa within the phylum *Bacteroidota*, including species of the genera *Phocaeicola* (formerly *Bacteroides*), *Parabacteroides, Alistipes*, and *Odoribacter*. In contrast, important members of the phylum *Bacillota*, including *Blautia* and butyrate producers such as *Agathobacter*, *Coprococcus*, *Butyribacter*, *A. hallii* (formerly *Eubacterium hallii*), and *Anaerostipes* were reduced in PCC. Butyrate producers are considered to be beneficial to the host's health, and their reduction has been found to be linked to various diseases (Guilloteau et al. 2010; Pozuelo et al. 2015; Noureldein et al. 2020). A multi-omics study in COVID-19 patients observed a disturbed immunological defense in the gut mucosa, which manifested in a reduction of host anti-bacteria immunoglobulins leading to reduction in butyrate producers, which could affect the long-term gut immune response in PCC (He et al. 2021).

We then investigated whether these microbiota shifts were associated with risk factors and typical symptoms known to occur in PCC. Risk factors for the development of PCC like diabetes were associated with a decrease in relative abundance of *B. faecis* and *A. hallii*, both linked to a healthy phenotype and better glucose tolerance in Type 2 diabetes studies (Daskova et al. 2023; Perraudeau et al. 2020). Although varying in their findings, previous studies have reported microbial alterations to be associated with different PCC symptoms (Liu et al. 2022; Su et al. 2024; Vestad et al. 2022). Liu et al. performed one of the largest microbiome studies in PCC ($N = 106$) and found a depletion of the species *Ruminococcus inulinivorans* and *Faecalibacterium prausnitzii* to be linked to hair loss, whereas *Clostridium innocuum* and *Actinomyces naeslundii* were linked to fatigue and neuropsychiatric symptoms (Liu et al. 2022). While associations to affective symptomatology based on HADS score were limited, our correlation analysis revealed that increased relative abundance of *B. wadsworthia* was associated with higher PSQI and FSMC scores, which indicated a poor sleep quality and fatigue in our cohort.

*B. wadsworthia* has also been found to play an important role in inflammation and gut barrier dysfunction (Feng et al. 2017;



20404603, 2026, 5, Downloaded from https://onlinelibrary.wiley.com/doi/10.1002/cph4.70261 by Universitatsbibliothek RWTH Aachen University, Wiley Online Library on [13/11/2026]. See the Terms and Conditions (https://onlinelibrary.wiley.com/terms-and-conditions) on Wiley Online Library for rules of use; OA articles are governed by the applicable Creative Commons License

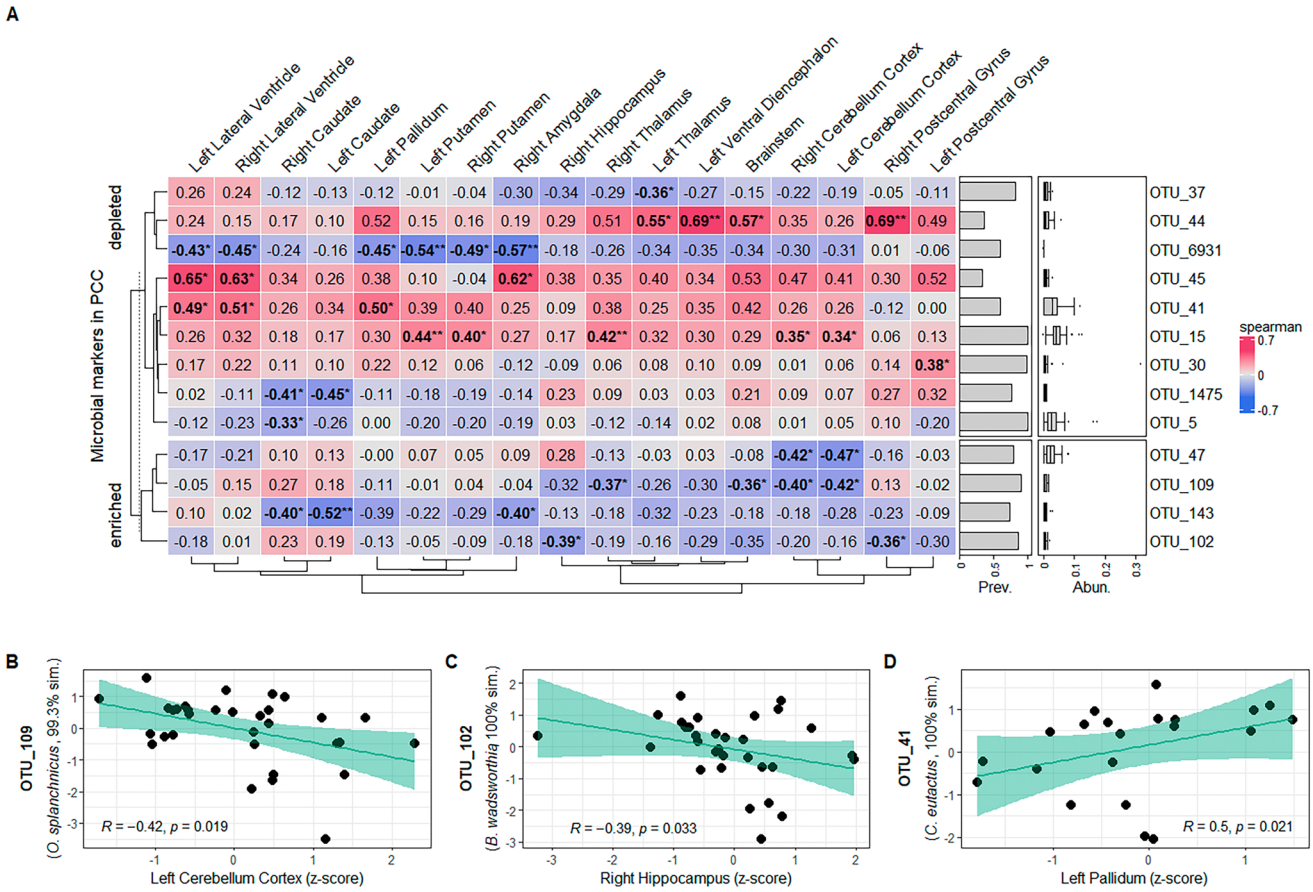



**FIGURE 4** | Correlation analysis results from center-log ratio transformed, relative abundance of microbial taxa and structural brain changes in the PCC cohort. (A) Heatmap showing spearman correlation coefficients and indicating unadjusted significance levels (*$p < 0.05$, **$p < 0.01$). (B–D) Linear regression plots highlighting the associations between *O. splanchnicus* (OTU_109) and left cerebellum cortex, *B. wadsworthia* (OTU_102) and right hippocampus, and *C. eutactus* (OTU_41) and left pallidum, respectively.

Devkota et al. 2012). In addition, a recent study found microbe-microbe interaction between *B. wadsworthia* and *Bacteroides thetaiotaomicron* to exacerbate a pro-inflammatory state in the human gut, with *B. thetaiotaomicron* (OTU_469) also being enriched in our PCC cohort (Davies et al. 2024). It has also been found to be increased in patients with Parkinson's disease, implying a potential association with neurological health (Baldini et al. 2020; Zhao et al. 2024).

To investigate, whether gut microbiota changes were also associated with brain parameters, we proceeded by correlating the abundances of the relevant genera with structural and functional brain changes measured in MRI imaging, focusing on regions we have previously identified to be affected within the present PCC cohort (Dadsena, Walders, et al. 2025; Dadsena, Wetz, et al. 2025). We found associations between the nucleus caudatus and the amygdala, and the relative abundance of *A. communis*. This is remarkable as the genus of *Alistipes* has previously been linked to Myalgic Encephalitis/Chronic Fatigue Syndrome, the most severe form of PCC, and to psychiatric diseases including, major depression disorder and anxiety during lockdown (Fremont et al. 2013; Bangsgaard Bendtsen et al. 2012; Jiang et al. 2015; Sik Novak et al. 2022). Similarly, we also found wider brain associations for *O. splanchnicus*. It was negatively associated with volumes of the cerebellar cortex, the thalamus and the brainstem, supporting our hypothesis that microbiome alterations in PCC could affect vagal pathways via the brainstem, as previously proposed by others (Radke et al. 2024). Although a previous multi-center study linked the genus of *Odoribacter* to preserved cognition and greater hippocampal volume, our PCC cohort showed higher relative abundances of *O. splanchnicus* and no association with the hippocampus (Liang et al. 2022). This contrast may be associated with differences in the inflammatory and immunometabolic environment in PCC, although its relationship with microbial function and host-microbiome signaling remains unclear. However, our finding further underscores the strong link between *Odoribacter* and cerebral structures, although its effects may differ across disease states. We found more localized associations between *C. eutactus* and the pallidum, as well as the lateral ventricles. *C. eutactus* has previously been studied in animal models and found to have an attenuating effect on depression-like behavior and affect neurotransmitter metabolism (Xu et al. 2024). The observation that some taxa were associated with multiple brain regions, while others correlated with only one or two, could point towards differential regional sensitivity to systemic influences such as immune activation, metabolic alterations, or neurotransmitter modulation, which may be affected by gut microbiota and warrant further investigation. As such, brain



20404603, 2026, 5, Downloaded from https://onlinelibrary.wiley.com/doi/10.1002/cph4.70261 by Universitatsbibliothek RWTH Aachen University, Wiley Online Library on [13/11/2026]. See the Terms and Conditions (https://onlinelibrary.wiley.com/terms-and-conditions) on Wiley Online Library for rules of use; OA articles are governed by the applicable Creative Commons License

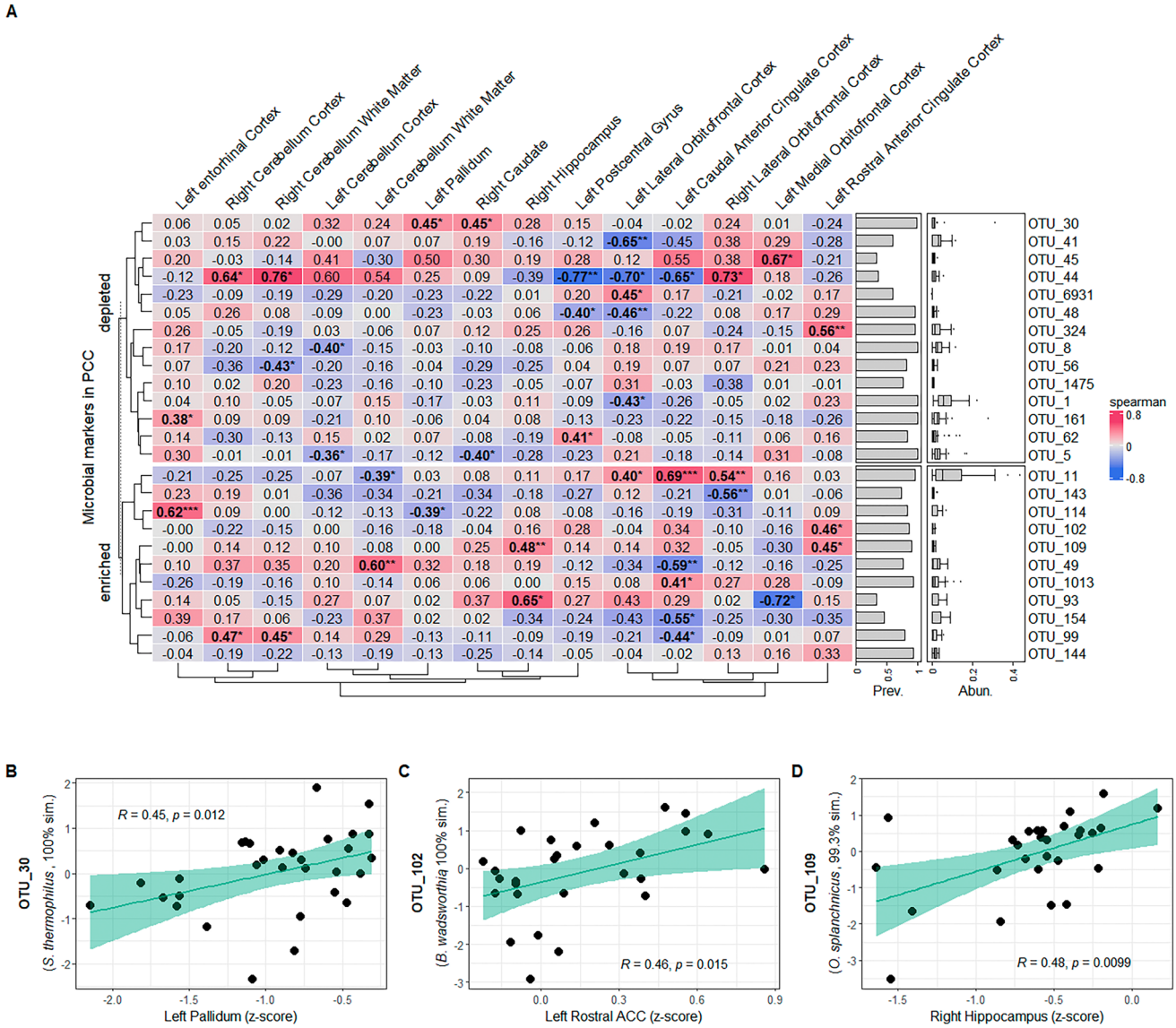



**FIGURE 5** | Correlation analysis results from center-log ratio transformed, relative abundance of microbial taxa and functional brain changes in the PCC cohort. (A) Heatmap showing spearman correlation coefficients and indicating unadjusted significance levels (*$p < 0.05$, **$p < 0.01$, ***$p < 0.001$). (B–D) Linear regression plots highlighting the associations between *S. thermophilus* (OTU_30) and left pallidum, *B. wadsworthia* (OTU_102) and left rostral ACC (Anterior Cingulate Cortex), and *O. splanchnicus* (OTU_109) and right hippocampus, respectively.

regions like the pallidum and the cerebellar cortex, could be particularly vulnerable to such changes due to their high metabolic demand and dense microglial populations.

On a functional level, brain changes in the pallidum and nucleus caudatus were correlated with *S. thermophilus*, which was associated with the healthy control group and depleted in PCC patients. One study found *S. thermophilus* to reverse depression-like behaviors and control stress in mice through ammonia production, hinting at a positive effect on the gut-brain axis reduced in PCC (Wang et al. 2023). In addition, *R. callidus*, depleted in PCC and found to be reduced in patients with inflammatory bowel disease, was not only associated with several brain regions including the cerebellum and orbital frontal areas, but also with measures of sleep, fatigue, affective symptoms, and IL-8 (Kang et al. 2010). Regarding neuronal injury markers, we observed some positive associations of NfL and GFAP with protective taxa reduced in PCC. However, interpretation of these associations remains largely speculative, given that GFAP levels were within the reference range when compared with age-matched mean values reported in the literature (Tybirk et al. 2022).

Taken together, our correlation analyses revealed that distinct taxa correlated with clinical symptoms and brain changes such as *B. wadsworthia and R. callidus*. Other taxa were more specifically associated with brain alterations, such as *S. thermophilus*, suggesting separate pathways of microbiota-brain interaction via the gut-brain axis in PCC. Overall, the observed associations may reflect relationships between symptom-related taxa and immune or metabolic mechanisms, and between brain-associated taxa and neuroinflammatory or neurodegenerative processes, although the underlying mechanisms remain uncertain. The major strength of our study lies in the concurrent availability of



20404603, 2026, 5, Downloaded from https://onlinelibrary.wiley.com/doi/10.1002/cph4.70261 by Universitatsbibliothek RWTH Aachen University, Wiley Online Library on [13/11/2026]. See the Terms and Conditions (https://onlinelibrary.wiley.com/terms-and-conditions) on Wiley Online Library for rules of use; OA articles are governed by the applicable Creative Commons License

gut microbiota and MRI data in PCC patients. This enabled us to conduct a comprehensive, end-to-end investigation of gut–brain associations in PCC, allowing us to identify potential underlying targets worth investigating in further studies. Given that our study focused on a neurologically characterized cohort, we were able to adopt a more targeted analysis on key PCC symptoms, particularly fatigue and cognitive dysfunction, compared to previous microbiome studies. Nevertheless, limitations include the cross-sectional design, the small sample size and the reliance on two distinct control groups assessed at different timepoints. Thus, conclusions drawn from our analysis remain associative. Larger sample size studies with a control group recruited in parallel for MRI and microbiome data and ideally supplemented with metabolomic data, will be needed to consolidate findings and explore the causal relationship between shifts in gut microbiota composition and changes at the brain level. In addition, due to the usage of an external healthy control group, possible batch effects could have occurred.

In conclusion, this exploratory study provides first hints at significant gut microbiota alterations and potentially affected mechanisms in PCC patients with predominantly neurological symptoms. These alterations were linked not only to clinical symptoms but also to changes in brain structure and function, underscoring the need for interventional studies to evaluate potential benefits of microbiota-targeted approaches for neurological symptoms and brain recovery in PCC.

### Author Contributions

Conception and design of the study: Kathrin Reetz, Julia Walders, Sophie Wetz. Acquisition of data: Julia Walders, Sophie Wetz, Ana S. Costa, Thomas Clavel, Nicole Treichel, Anna Hofmann. Sophie Wetz and Nicole Treichel carried out microbiota analysis. Previous MRI analysis: Ravi Dadsena. Formal analysis: Sophie Wetz. Writing – Original Draft: Sophie Wetz. Visualization: Sophie Wetz. Supervision: Julia Walders. Funding acquisition: Julia Walders. Project administration: Julia Walders. All authors have reviewed and approved the manuscript.


### Acknowledgments

This work was supported by the Brain Imaging Facility of the Interdisciplinary Center for Clinical Research (IZKF) Aachen within the Faculty of Medicine at RWTH Aachen University. Open Access funding enabled and organized by Projekt DEAL.

### Funding

This research project was supported by the Clinician Scientist Program of the Faculty of Medicine RWTH Aachen University to JW. The research project is supported by the Else-Kröner-Fresenius Stiftung to JW (Grant 2022_EKEA.58). TC received funding from the German Research Foundation (DFG), project no. 403224013–SFB1382.


### Ethics Statement

Approval for all procedures was obtained from the local ethics committee ("Ethikkommission an der Medizinischen Fakultät der RWTH Aachen") and followed the Declaration of Helsinki (EK 192/20).

### Consent

All individuals gave written informed consent before participating in the study.

### Conflicts of Interest

The authors declare no conflicts of interest.

### Data Availability Statement

Raw 16S rRNA gene amplicon data are available at the European Nucleotide Archive/NCBI under BioProject accession number PRJEB108715.

### References


Afrizal, A., T. C. A. Hitch, A. Viehof, et al. 2022. "Anaerobic Single-Cell Dispensing Facilitates the Cultivation of Human Gut Bacteria." *Environmental Microbiology* 24: 3861–3881.

Aitchison, J. 1982. "The Statistical Analysis of Compositional Data." *Journal of the Royal Statistical Society. Series B, Methodological* 44: 139–177.

Aschenbrenner, S., O. Tucha, and K. W. Lange. 2000. "RWT: Regensburger Wortflüssigkeits-Test." Hogrefe.

Baldini, F., J. Hertel, E. Sandt, et al. 2020. "Parkinson's Disease-Associated Alterations of the Gut Microbiome Predict Disease-Relevant Changes in Metabolic Functions." *BMC Biology* 18: 62.

Bangsgaard Bendtsen, K. M., L. Krych, D. B. Sørensen, et al. 2012. "Gut Microbiota Composition Is Correlated to Grid Floor Induced Stress and Behavior in the BALB/c Mouse." *PLoS One* 7: e46231.

Barnett, D., I. Arts, and J. Penders. 2021. "microViz: An R Package for Microbiome Data Visualization and Statistics." *Journal of Open Source Software* 6: 3201.

Bäumler, G. 1985. "Farbe-Wort-Interferenztest (FWIT) Nach J. R. Stroop."

Bungenberg, J., C. Hohenfeld, A. S. Costa, et al. 2024. "Characteristic Functional Connectome Related to Post-COVID-19 Syndrome." *Scientific Reports* 14: 4997.

Bungenberg, J., K. Humkamp, C. Hohenfeld, et al. 2022. "Long COVID-19: Objectifying Most Self-Reported Neurological Symptoms." *Annals of Clinical Translational Neurology* 9: 141–154.

Cao, Y., Q. Dong, D. Wang, P. Zhang, Y. Liu, and C. Niu. 2022. "microbiomeMarker: An R/Bioconductor Package for Microbiome Marker Identification and Visualization." *Bioinformatics* 38: 4027–4029.

Chalita, M., Y. O. Kim, S. Park, et al. 2024. "EzBioCloud: A Genome-Driven Database and Platform for Microbiome Identification and Discovery." *International Journal of Systematic and Evolutionary Microbiology* 74: 006421.

Cryan, J. F., K. J. O'Riordan, C. S. M. Cowan, et al. 2019. "The Microbiota-Gut-Brain Axis." *Physiological Reviews* 99: 1877–2013.

Dadsena, R., J. Walders, A. S. Costa, et al. 2025. "Two-Year Impact of COVID-19: Longitudinal MRI Brain Changes and Neuropsychiatric Trajectories." *Psychiatry and Clinical Neurosciences* 79: 176–186.

Dadsena, R., S. Wetz, A. Hofmann, et al. 2025. "Evidence of Clinical and Brain Recovery in Post-COVID-19 Condition: A Three-Year Follow-Up Study." *Brain Communication* 7: fcaf366.

Daskova, N., I. Modos, M. Krbcová, et al. 2023. "Multi-Omics Signatures in New-Onset Diabetes Predict Metabolic Response to Dietary Inulin: Findings From an Observational Study Followed by an Interventional Trial." *Nutrition & Diabetes* 13: 7.

Davies, J., M. J. Mayer, N. Juge, A. Narbad, and L. Sayavedra. 2024. "Bacteroides Thetaiotaomicron Enhances H(2)S Production in *Bilophila wadsworthia*." *Gut Microbes* 16: 2,431,644.

Davis, H. E., L. McCorkell, J. M. Vogel, and E. J. Topol. 2023. "Long COVID: Major Findings, Mechanisms and Recommendations." *Nature Reviews Microbiology* 21: 133–146.





20404603, 2026, 5, Downloaded from https://onlinelibrary.wiley.com/doi/10.1002/cph4.70261 by Universitatsbibliothek RWTH Aachen University, Wiley Online Library on [13/11/2026]. See the Terms and Conditions (https://onlinelibrary.wiley.com/terms-and-conditions) on Wiley Online Library for rules of use; OA articles are governed by the applicable Creative Commons License

Devkota, S., Y. Wang, M. W. Musch, et al. 2012. "Dietary-Fat-Induced Taurocholic Acid Promotes Pathobiont Expansion and Colitis in Il10−/− Mice." *Nature* 487: 104–108.

Douaud, G., S. Lee, F. Alfaro-Almagro, et al. 2022. "SARS-CoV-2 Is Associated With Changes in Brain Structure in UK Biobank." *Nature* 604: 697–707.

Edgar, R. C. 2010. "Search and Clustering Orders of Magnitude Faster Than BLAST." *Bioinformatics* 26: 2460–2461.

Edgar, R. C. 2013. "UPARSE: Highly Accurate OTU Sequences From Microbial Amplicon Reads." *Nature Methods* 10: 996–998.

Edgar, R. C., B. J. Haas, J. C. Clemente, C. Quince, and R. Knight. 2011. "UCHIME Improves Sensitivity and Speed of Chimera Detection." *Bioinformatics* 27: 2194–2200.

Elboraay, T., M. A. Ebada, M. Elsayed, et al. 2025. "Long-Term Neurological and Cognitive Impact of COVID-19: A Systematic Review and Meta-Analysis in Over 4 Million Patients." *BMC Neurology* 25: 250.

Feng, Z., W. Long, B. Hao, et al. 2017. "A Human Stool-Derived *Bilophila wadsworthia* Strain Caused Systemic Inflammation in Specific-Pathogen-Free Mice." *Gut Pathogens* 9: 59.

Fremont, M., D. Coomans, S. Massart, and K. De Meirleir. 2013. "High-Throughput 16S rRNA Gene Sequencing Reveals Alterations of Intestinal Microbiota in Myalgic Encephalomyelitis/Chronic Fatigue Syndrome Patients." *Anaerobe* 22: 50–56.

Guilloteau, P., L. Martin, V. Eeckhaut, R. Ducatelle, R. Zabielski, and F. van Immerseel. 2010. "From the Gut to the Peripheral Tissues: The Multiple Effects of Butyrate." *Nutrition Research Reviews* 23: 366–384.

Guilmette, T. J., J. J. Sweet, N. Hebben, et al. 2020. "American Academy of Clinical Neuropsychology Consensus Conference Statement on Uniform Labeling of Performance Test Scores." *Clinical Neuropsychologist* 34: 437–453.

Hastie, C. E., D. J. Lowe, A. McAuley, et al. 2023. "Natural History of Long-COVID in a Nationwide, Population Cohort Study." *Nature Communications* 14: 3504.

He, F., T. Zhang, K. Xue, et al. 2021. "Fecal Multi-Omics Analysis Reveals Diverse Molecular Alterations of Gut Ecosystem in COVID-19 Patients." *Analytica Chimica Acta* 1180: 338881.

Heine, J., K. Schwichtenberg, T. J. Hartung, et al. 2023. "Structural Brain Changes in Patients With Post-COVID Fatigue: A Prospective Observational Study." *EClinicalMedicine* 58: 101874.

Herrmann, C., and U. Buss. 1994. "Vorstellung Und Validierung Einer Deutschen Version der "Hospital Anxiety and Depression Scale"(HAD-Skala){Description and Validation of a German Version of the Hospital Anxiety and Depression (HAD) Scale}." *Diagnostica* 40: 143–154.

Hossain, B., F. Malik, A. Khan, et al. 2023. "Prevalence and Impact of Gastrointestinal Manifestations in COVID-19 Patients: A Systematic Review." *Journal of Community Hospital Internal Medicine Perspectives* 13: 39–54.

Jiang, H., Z. Ling, Y. Zhang, et al. 2015. "Altered Fecal Microbiota Composition in Patients With Major Depressive Disorder." *Brain, Behavior, and Immunity* 48: 186–194.

Jones, D. L., M. Q. Baluja, D. W. Graham, et al. 2020. "Shedding of SARS-CoV-2 in Feces and Urine and Its Potential Role in Person-To-Person Transmission and the Environment-Based Spread of COVID-19." *Science of the Total Environment* 749: 141364.

Kang, S., S. E. Denman, M. Morrison, et al. 2010. "Dysbiosis of Fecal Microbiota in Crohn's Disease Patients as Revealed by a Custom Phylogenetic Microarray." *Inflammatory Bowel Diseases* 16: 2034–2042.

Lagkouvardos, I., S. Fischer, N. Kumar, and T. Clavel. 2017. "*rhea*: A Transparent and Modular R Pipeline for Microbial Profiling Based on 16S rRNA Gene Amplicons." *PeerJ* 5: e2836.

Lagkouvardos, I., D. Joseph, M. Kapfhammer, et al. 2016. "IMNGS: A Comprehensive Open Resource of Processed 16S rRNA Microbial Profiles for Ecology and Diversity Studies." *Scientific Reports* 6: 33,721.

Lau, R. I., Q. Su, and S. C. Ng. 2025. "Long COVID and Gut Microbiome: Insights Into Pathogenesis and Therapeutics." *Gut Microbes* 17: 2,457,495.

Liang, X., Y. Fu, W. T. Cao, et al. 2022. "Gut Microbiome, Cognitive Function and Brain Structure: A Multi-Omics Integration Analysis." *Transl Neurodegener* 11: 49.

Liu, Q., J. W. Y. Mak, Q. Su, et al. 2022. "Gut Microbiota Dynamics in a Prospective Cohort of Patients With Post-Acute COVID-19 Syndrome." *Gut* 71: 544–552.

McMurdie, P. J., and S. Holmes. 2013. "Phyloseq: An R Package for Reproducible Interactive Analysis and Graphics of Microbiome Census Data." *PLoS One* 8: e61217.

Nasreddine, Z. S., N. A. Phillips, V. Bédirian, et al. 2005. "The Montreal Cognitive Assessment, MoCA: A Brief Screening Tool for Mild Cognitive Impairment." *Journal of the American Geriatrics Society* 53: 695–699.

Natarajan, A., S. Zlitni, E. F. Brooks, et al. 2022. "Gastrointestinal Symptoms and Fecal Shedding of SARS-CoV-2 RNA Suggest Prolonged Gastrointestinal Infection." *Medicus* 3: 371–387.

Noureldein, M. H., S. Bitar, N. Youssef, S. Azar, and A. A. Eid. 2020. "Butyrate Modulates Diabetes-Linked Gut Dysbiosis: Epigenetic and Mechanistic Modifications." *Journal of Molecular Endocrinology* 64: 29–42.

Oksanen, J., F. Blanchet, R. Kindt, et al. 2022. "Vegan: Community Ecology Package." https://vegandevs.github.io/vegan/.

Paužuolis, M., D. Fatykhova, B. Zühlke, et al. 2024. "SARS-CoV-2 Tropism to Intestinal but Not Gastric Epithelial Cells Is Defined by Limited ACE2 Expression." *Stem Cell Reports* 19: 629–638.

Penner, I. K., C. Raselli, M. Stöcklin, K. Opwis, L. Kappos, and P. Calabrese. 2009. "The Fatigue Scale for Motor and Cognitive Functions (FSMC): Validation of a New Instrument to Assess Multiple Sclerosis-Related Fatigue." *Multiple Sclerosis* 15: 1509–1517.

Perraudeau, F., P. McMurdie, J. Bullard, et al. 2020. "Improvements to Postprandial Glucose Control in Subjects With Type 2 Diabetes: A Multicenter, Double Blind, Randomized Placebo-Controlled Trial of a Novel Probiotic Formulation." *BMJ Open Diabetes Research & Care* 8: e001319.

Petermann, F. 2014. "Wechsler Adult Intelligence Scale-: Deutschsprachige Adaptation der WAIS-IV von D. Wechsler." Pearson.

Pozuelo, M., S. Panda, A. Santiago, et al. 2015. "Reduction of Butyrate- and Methane-Producing Microorganisms in Patients With Irritable Bowel Syndrome." *Scientific Reports* 5: 12,693.

Price, M. N., P. S. Dehal, and A. P. Arkin. 2010. "FastTree 2–Approximately Maximum-Likelihood Trees for Large Alignments." *PLoS One* 5: e9490.

Pruesse, E., J. Peplies, and F. O. Glockner. 2012. "SINA: Accurate High-Throughput Multiple Sequence Alignment of Ribosomal RNA Genes." *Bioinformatics* 28: 1823–1829.

Radke, J., J. Meinhardt, T. Aschman, et al. 2024. "Proteomic and Transcriptomic Profiling of Brainstem, Cerebellum and Olfactory Tissues in Early- and Late-Phase COVID-19." *Nature Neuroscience* 27: 409–420.

Reitmeier, S., T. C. A. Hitch, N. Treichel, et al. 2021. "Handling of Spurious Sequences Affects the Outcome of High-Throughput 16S rRNA Gene Amplicon Profiling." *ISME Communications* 1: 31.

Rua, C., B. Raman, C. T. Rodgers, et al. 2024. "Quantitative Susceptibility Mapping at 7T in COVID-19: Brainstem Effects and Outcome Associations." *Brain* 147: 4121–4130.



20404603, 2026, 5, Downloaded from https://onlinelibrary.wiley.com/doi/10.1002/cph4.70261 by Universitatsbibliothek RWTH Aachen University, Wiley Online Library on [13/11/2026]. See the Terms and Conditions (https://onlinelibrary.wiley.com/terms-and-conditions) on Wiley Online Library for rules of use; OA articles are governed by the applicable Creative Commons License

Russ, M. 2001. "Normierung und Validierung des Frankfurter Neuropsychologischen Testprofils." *Thesis*.

Schmiester, M., R. Maier, R. Riedel, et al. 2022. "Flow Cytometry Can Reliably Capture Gut Microbial Composition in Healthy Adults as Well as Dysbiosis Dynamics in Patients With Aggressive B-Cell Non-Hodgkin Lymphoma." *Gut Microbes* 14: 2081475.

Segata, N., J. Izard, L. Waldron, et al. 2011. "Metagenomic Biomarker Discovery and Explanation." *Genome Biology* 12: R60.

Sik Novak, K., N. Bogataj Jontez, S. Kenig, et al. 2022. "The Effect of COVID-19 Lockdown on Mental Health, Gut Microbiota Composition and Serum Cortisol Levels." *Stress* 25: 246–257.

Su, Q., R. I. Lau, Q. Liu, F. K. L. Chan, and S. C. Ng. 2023. "Post-Acute COVID-19 Syndrome and Gut Dysbiosis Linger Beyond 1 Year After SARS-CoV-2 Clearance." *Gut* 72: 1230–1232.

Su, Q., R. I. Lau, Q. Liu, et al. 2024. "The Gut Microbiome Associates With Phenotypic Manifestations of Post-Acute COVID-19 Syndrome." *Cell Host & Microbe* 32: 651–660.

Tombaugh, T. N. 2004. "Trail Making Test A and B: Normative Data Stratified by Age and Education." *Archives of Clinical Neuropsychology* 19: 203–214.

Tseng, C. H., and C. Y. Wu. 2019. "The Gut Microbiome in Obesity." *Journal of the Formosan Medical Association* 118, no. Suppl 1: S3–S9.

Tybirk, L., C. V. B. Hviid, C. S. Knudsen, and T. Parkner. 2022. "Serum GFAP—Reference Interval and Preanalytical Properties in Danish Adults." *Clinical Chemistry and Laboratory Medicine* 60: 1830–1838.

Vakil, E., Y. Greenstein, and H. Blachstein. 2010. "Normative Data for Composite Scores for Children and Adults Derived From the Rey Auditory Verbal Learning Test." *Clinical Neuropsychologist* 24: 662–677.

Vestad, B., T. Ueland, T. V. Lerum, et al. 2022. "Respiratory Dysfunction Three Months After Severe COVID-19 Is Associated With Gut Microbiota Alterations." *Journal of Internal Medicine* 291: 801–812.

Wang, P., P. F. Wu, H. J. Wang, F. Liao, F. Wang, and J. G. Chen. 2023. "Gut Microbiome-Derived Ammonia Modulates Stress Vulnerability in the Host." *Nature Metabolism* 5: 1986–2001.

Wong, A. C., A. S. Devason, I. C. Umana, et al. 2023. "Serotonin Reduction in Post-Acute Sequelae of Viral Infection." *Cell* 186: 4851–4867.

Xu, L., S. Wang, L. Wu, et al. 2024. "*Coprococcus eutactus* Screened From Healthy Adolescent Attenuates Chronic Restraint Stress-Induced Depression-Like Changes in Adolescent Mice: Potential Roles in the Microbiome and Neurotransmitter Modulation." *Journal of Affective Disorders* 356: 737–752.

Yeoh, Y. K., T. Zuo, G. C. Y. Lui, et al. 2021. "Gut Microbiota Composition Reflects Disease Severity and Dysfunctional Immune Responses in Patients With COVID-19." *Gut* 70: 698–706.

Zhao, Z., J. Chen, D. Zhao, et al. 2024. "Microbial Biomarker Discovery in Parkinson's Disease Through a Network-Based Approach." *NPJ Parkinsons Disease* 10: 203.

Zhou, Y., J. Chi, W. Lv, and Y. Wang. 2021. "Obesity and Diabetes as High-Risk Factors for Severe Coronavirus Disease 2019 (Covid-19)." *Diabetes/Metabolism Research and Reviews* 37: e3377.

Zhou, Z., B. Sun, D. Yu, and C. Zhu. 2022. "Gut Microbiota: An Important Player in Type 2 Diabetes Mellitus." *Frontiers in Cellular and Infection Microbiology* 12: 834,485.

Zimmermann, P., and B. Fimm. 2017. "Testbatterie zur Aufmerksamkeitsprüfung (TAP 2.3. 1)." Psychologische Testsysteme.

## Supporting Information

Additional supporting information can be found online in the Supporting Information section. **Figure S1:** Study cohort reported symptoms and neuropsychological test results. (A) Count of participants' self-reported symptoms and characteristics. (B) Study cohort's neuropsychological test performance. Dark shade indicates normal performance, middle shade indicates a performance between the 2nd and 16th percent range, while light shade indicates a performance < 2% compared to normative data. The test categories are indicated by color. **Figure S2:** Correlation analysis results from center-log ratio transformed relative abundance of microbial markers and clinical variables in the PCC study cohort. The heatmap shows pearson correlation coefficients for reported symptoms and microbial markers and indicating unadjusted significance levels ($*p < 0.05$, $**p < 0.01$). **Figure S3:** Correlation analysis results from center-log ratio transformed relative abundance of microbial markers and neuropsychological test results in the PCC study cohort. The heatmap shows spearman correlation coefficients with asterisks indicating unadjusted significance levels ($*p < 0.05$, $**p < 0.01$). **Figure S4:** Study design overview. Green indicates data collected within the PCC cohort, while blue indicates healthy control data used for MRI analysis (from pre-pandemic register studies at the University Hospital Aachen) or for 16S rRNA gene amplicon sequencing (publicly available data, collected before the COVID-19 pandemic, from a study by Schmiester et al. at Charité Berlin).



20404603, 2026, 5, Downloaded from https://onlinelibrary.wiley.com/doi/10.1002/cph4.70261 by Universitatsbibliothek RWTH Aachen University, Wiley Online Library on [13/11/2026]. See the Terms and Conditions (https://onlinelibrary.wiley.com/terms-and-conditions) on Wiley Online Library for rules of use; OA articles are governed by the applicable Creative Commons License